Supporting Information for:

Embedded Cluster Model for Al_2O_3 and $AlPO_4$ Surfaces Using Point Charges and Periodic Electrostatic Potential

Masafuyu Matsui[§] and Shigeyoshi Sakaki*[§¶]

[§] Elements Strategy Initiative for Catalysts and Batteries (ESICB), Kyoto University, 1-30 Goryo-Ohara, Nishikyo-ku, Kyoto 615-8245, Japan
[¶] Fukui Institute for Fundamental Chemistry, Kyoto University, Nishi-hiraki-cho 34-4, Takano, Sakyo-ku, Kyoto 606-8103, Japan

E-mail: sakaki.shigeyoshi.47e@st.kyoto-u.ac.jp

Contents

Complete Reference

81. Frisch, M. J.; Trucks, G. W.; Schlegel, H. B.; Scuseria, G. E.; Robb, M. A.; Cheeseman, J. R.; Scalmani, G.; Barone, V.; Mennucci, B.; Petersson, G. A.; Nakatsuji, H.; Caricato, M.; Li, X.; Hratchian, H. P.; Izmaylov, A. F.; Bloino, J.; Zheng, G.; Sonnenberg, J. L.; Hada, M.; Ehara, M.; Toyota, K.; Fukuda, R.; Hasegawa, J.; Ishida, M.; Nakajima, T.; Honda, Y.; Kitao, O.; Nakai, H.; Vreven, T.; Montgomery, Jr., J. A.; , Peralta, J. E.; Ogliaro, F.; Bearpark, M.; Heyd, J. J.; Brothers, E.; Kudin, K. N.; Staroverov, V. N.; Keith, T.; Kobayashi, R.; Normand, J.; Raghavachari, K.; Rendell, A.; Burant, J. C.; Iyengar, S. S.; Tomasi, J.; Cossi, M.; Rega, N.; Millam, J. M.; Klene, M.; Knox, J. E.; Cross, J. B.; Bakken, V.; Adamo, C.; Jaramillo, J.; Gomperts, R.; Stratmann, R. E.; Yazyev, O.; Austin, A. J.; Cammi, R.; Pomelli, C.; Ochterski, J. W.; Martin, R. L.; Morokuma, K.; Zakrzewski, V. G.; Voth, G. A.; Salvador, P.; Dannenberg, J. J.; Dapprich, S.; Daniels, A. D.; Farkas, O.; Foresman, J. B.; Ortiz, J. V.; Cioslowski, J.; Fox, D. J. *Gaussian 09, Revision D.01*, Gaussian, Inc., Wallingford CT 2013.

Derivation of One-electron Integral of Periodic Electrostatic Potential

The one way to incorporate the electrostatic potential by the bulk is to use electrostatic potential that is calculated using periodic PC distribution obtained by slab calculation. Here, we describe how to construct such electrostatic potential embedding method.

Because Gaussian basis functions are employed in almost all cluster models, we need to calculate one-electron integral of periodic point charge distribution, using Gaussian basis functions. Under the periodic boundary condition (PBC), one-electron orbital $\psi_{i,\mathbf{k}}(\mathbf{r})$ is represented by a Bloch function, as follows:

$$\psi_{i,\mathbf{k}}(\mathbf{r}) = u_{i,\mathbf{k}}(\mathbf{r})\, e^{i\mathbf{k}\cdot\mathbf{r}} \tag{S1}$$

where i, $\mathbf{k}$, and $u_{i,\mathbf{k}}$ are a band index, a wave vector, and a periodic part of the Bloch function, respectively. The periodic part $u_{i,\mathbf{k}}$ is represented by a linear combination of periodic Gaussian basis functions $\phi^{\mathrm{PBC}}_{An,\mathbf{k}}$; see eqs. S2 and S3;

$$u_{i,\mathbf{k}}(\mathbf{r}) = \sum_{An} C_{An\,i,\mathbf{k}}\, \phi^{\mathrm{PBC}}_{An,\mathbf{k}}(\mathbf{r}) \tag{S2}$$

$$\phi^{\mathrm{PBC}}_{An,\mathbf{k}}(\mathbf{r}) = \sum_{\mathbf{R}} \phi_{An}(\mathbf{r}-\mathbf{R}) e^{i\mathbf{k}\cdot\mathbf{R}} \tag{S3}$$

where $\mathbf{R}$ is a lattice vector, $C_{Ani,\mathbf{k}}$ is a coefficient of linear combination, and ϕ_{An} is a contracted Gaussian basis function at $\mathbf{r}_A = (x_A, y_A, z_A)$, and A and n are indices of atom and basis function at $\mathbf{r}_A$, respectively. The basis function ϕ_{An} is given by Cartesian Gaussian function φ_{Aal};

$$\phi_{An}(\mathbf{r}) = \sum_{a} N_{al} c_{an}\, \varphi_{Aal}(\mathbf{r}) \tag{S4}$$

where N_{al} is a normalization constant, c_{an} is a contraction coefficient, and l is a total angular momentum. The Cartesian Gaussian function φ_{Aal} is given by eq. S5;

$$\begin{aligned}\varphi_{Aal}(\mathbf{r}) &= (x-x_A)^{l_x}(y-y_A)^{l_y}(z-z_A)^{l_z} \exp\left(-\alpha_a|\mathbf{r}-\mathbf{r}_A|^2\right) \\ &= (x-x_A)^{l_x}(y-y_A)^{l_y}(z-z_A)^{l_z}\, g_{Aa}(\mathbf{r})\end{aligned} \tag{S5}$$

where l_x, l_y, and l_z are Cartesian angular momenta of x, y, and z components, respectively, and g_{Aa} is a primitive Gaussian function at $\mathbf{r}_A$.

Here, we employed the super-cell approach,[S1] where each cluster is positioned in one unit cell with very large lattice vectors, and the centers of basis functions are placed in the same cell; these are possible without loss of generality. Because the cluster and its periodic images are separated very well from each other under this condition, overlap between basis functions of the clusters located at different cells is negligibly small;

$$\phi_{An}(\mathbf{r}-\mathbf{R})\,\phi_{Bm}(\mathbf{r}-\mathbf{R}') \approx 0 \quad (\mathbf{R} \neq \mathbf{R}') \tag{S6}$$

Owing to the sufficient separation of the clusters, band dispersion disappears, and only the Γ-point ($\mathbf{k}$ = (0, 0, 0)) sampling over the first Brillouin zone is necessary.

Under such conditions, the one-electron orbital ψ_i of the cluster model is represented by eq. S7;

$$\psi_i(\mathbf{r}) = \sum_{An} C_{An\,i}\phi_{An}^{\mathrm{PBC}}(\mathbf{r}) \tag{S7}$$

The basis function ϕ_{An}^{PBC} can be represented with Cartesian Gaussian function (eq. S5) by eq. 8;

$$\begin{aligned}\phi_{An}^{\mathrm{PBC}}(\mathbf{r}) &= \sum_{a} N_{al}c_{an}\,\varphi_{Aal}^{\mathrm{PBC}}(\mathbf{r}) \\ &= \sum_{a} N_{al}c_{an}\sum_{\mathbf{R}}\varphi_{Aal}(\mathbf{r}-\mathbf{R})\end{aligned} \tag{S8}$$

The next task is to evaluate one-electron integral of periodic potential;

$$\begin{aligned}\langle\phi_{An}^{\mathrm{PBC}}|\hat{V}^{\mathrm{PBC}}|\phi_{Bm}^{\mathrm{PBC}}\rangle &= \frac{1}{V^{\mathrm{SC}}}\int_{V^{\mathrm{SC}}} d\mathbf{r}\;\phi_{An}^{\mathrm{PBC}}(\mathbf{r})V^{\mathrm{PBC}}(\mathbf{r})\phi_{Bm}^{\mathrm{PBC}}(\mathbf{r}) \\ &= \sum_{a}\sum_{b} N_{al}N_{bl'}c_{a\,n}c_{b\,m}\frac{1}{V^{\mathrm{SC}}}\int_{V^{\mathrm{SC}}} d\mathbf{r}\;\varphi_{Aal}^{\mathrm{PBC}}(\mathbf{r})V^{\mathrm{PBC}}(\mathbf{r})\varphi_{Bbl'}^{\mathrm{PBC}}(\mathbf{r})\end{aligned} \tag{S9}$$

where V^{SC} is a volume of the super-cell and $\int_{V^{\mathrm{SC}}}d\mathbf{r}$ indicates integration over the super-cell. Because the overlap of basis functions between different cells can be neglected (see eq. S6), the integral in eq. S9 can be represented through Fourier transformation as follows:

$$\int_{V^{\mathrm{SC}}} d\mathbf{r}\;\varphi_{Aal}^{\mathrm{PBC}}(\mathbf{r})V^{\mathrm{PBC}}(\mathbf{r})\varphi_{Bbl'}^{\mathrm{PBC}}(\mathbf{r}) = \sum_{\mathbf{G}} V^{\mathrm{PBC}}(\mathbf{G})\int_{\mathrm{all}} d\mathbf{r}\;\varphi_{Aal}(\mathbf{r})\varphi_{Bbl'}(\mathbf{r})\,e^{i\mathbf{G}\cdot\mathbf{r}} \tag{S10}$$

where $V^{\mathrm{PBC}}(\mathbf{G})$ is a Fourier transform of $V^{\mathrm{PBC}}(\mathbf{r})$, $\mathbf{G}$ is a reciprocal lattice vector, and $\int_{\mathrm{all}}d\mathbf{r}$ indicates integration over all real-space.

The integral in the right-hand side in eq. S10 is a complex conjugate of Fourier transform of the product of two Cartesian Gaussian functions. To evaluate the one-electron integral of periodic potential, therefore, the Fourier transform of the product of two Cartesian Gaussian functions is required. Because both of the product of two Gaussian functions and the Fourier transform of Gaussian function are Gaussian function, the Fourier transform of the product of two Gaussian functions is also the Gaussian function as follows:

$$\int_{\text{all}} d\mathbf{r}\; g_{Aa}(\mathbf{r}) g_{Bb}(\mathbf{r})\, e^{-i\mathbf{G}\cdot\mathbf{r}} = \left(\frac{\pi}{\alpha_p}\right)^{\frac{3}{2}} F_{AaBb}\, e^{-i\mathbf{G}\cdot\mathbf{r}_P} \exp\left(-\frac{|\mathbf{G}|^2}{4\alpha_p}\right) \tag{S11}$$

where

$$\alpha_p = \alpha_a + \alpha_b, \quad F_{AaBb} = \exp\left(-\frac{\alpha_a\alpha_b}{\alpha_a+\alpha_b}|\mathbf{r}_A - \mathbf{r}_B|^2\right), \text{ and } \mathbf{r}_P = \frac{\alpha_a\mathbf{r}_A + \alpha_b\mathbf{r}_B}{\alpha_a+\alpha_b}$$

Though the Fourier transform of the product of two Cartesian Gaussian functions cannot be provided as a simple form, it can be represented as a recursion formula within a binomial expansion; details are presented in Appendix A (page S8)).

Hereafter, we focus on the electrostatic potential that is defined by eq. S12;

$$V^{\text{ES}}(\mathbf{r}) = \int_{\text{all}} d\mathbf{r}' \frac{n(\mathbf{r}')}{|\,\mathbf{r}-\mathbf{r}'\,|} + \sum_{\mathbf{R}}\sum_{C} \frac{Z_C}{|\,\mathbf{r}-\mathbf{r}_C-\mathbf{R}\,|} \tag{S12}$$

where $n(\mathbf{r})$ is electron density at $\mathbf{r}$ and Z_C is a nuclear charge of the C-th nucleus at $\mathbf{r}_C$ in the unit cell. Using Poisson's equation, $V^{\text{ES}}(\mathbf{r})$ is transformed to eq. S13;

$$V^{\text{ES}}(\mathbf{G}) = \frac{4\pi}{|\mathbf{G}|^2}\left(n(\mathbf{G}) + \sum_{C} Z_C e^{-i\mathbf{G}\cdot\mathbf{r}_C}\right) \tag{S13}$$

where $n(\mathbf{G})$ is a Fourier transform of $n(\mathbf{r})$. The one-electron integral of the electrostatic potential can be evaluated using eqs. S10 and S13; however, the Fourier series expansion in eq. S10 is, in general, not complete because the finite number of wave-vectors $\mathbf{G}$, which is usually determined by a cut-off energy, is not sufficient to incorporate high frequency components of the nuclear point-charge potential in reciprocal-space. To avoid this problem, the Ewald summation method, which is developed to evaluate electrostatic interaction between PCs in the PBC, is applied to evaluation of electrostatic interaction between PCs and one-electron orbital represented by the Gaussian basis functions in the PBC.

In the Ewald summation method, the electrostatic potential of PCs is represented as the sum of two short-range terms and one long-range term as follows:

$$V^{\mathrm{ES}}(\mathbf{r}) = V^{\mathrm{ES}}_{\mathrm{sr1}}(\mathbf{r}) + V^{\mathrm{ES}}_{\mathrm{sr2}}(\mathbf{r}) + V^{\mathrm{ES}}_{\mathrm{lr}}(\mathbf{r}) \tag{S14}$$

$$V^{\mathrm{ES}}_{\mathrm{sr1}}(\mathbf{r}) = \sum_{\mathbf{R},C}^{|\mathbf{r}-\mathbf{r}_C-\mathbf{R}|\le r_{\mathrm{cut}}} \frac{Z_C}{|\,\mathbf{r}-\mathbf{r}_C-\mathbf{R}\,|} \tag{S15}$$

$$V^{\mathrm{ES}}_{\mathrm{sr2}}(\mathbf{r}) = \sum_{\mathbf{R},C}^{|\mathbf{r}-\mathbf{r}_C-\mathbf{R}|\le r_{\mathrm{cut}}} \frac{-Z_C}{|\,\mathbf{r}-\mathbf{r}_C-\mathbf{R}\,|}\mathrm{erf}\left(\frac{1}{\sqrt{2}\sigma}|\mathbf{r}-\mathbf{r}_C-\mathbf{R}|\right) \tag{S16}$$

$$V^{\mathrm{ES}}_{\mathrm{lr}}(\mathbf{r}) = \sum_{\mathbf{G}}^{|\mathbf{G}|^2/2\le E_{\mathrm{cut}}} \frac{4\pi}{|\mathbf{G}|^2}\sum_C Z_C e^{-i\mathbf{G}\cdot\mathbf{r}_C}\exp\left(-\frac{\sigma^2|\mathbf{G}|^2}{2}\right)e^{i\mathbf{G}\cdot\mathbf{r}} \tag{S17}$$

where r_{cut} is a cut-off parameter in real-space, *erf* is an error function, σ is a convergence parameter of the Ewald sum, and E_{cut} is a cut-off energy in reciprocal space. Because the short-range terms have no reciprocal space contribution, one-electron integral of $V^{\mathrm{ES}}{}_{\mathrm{sr1}}$ can be evaluated in the same manner as nuclear-attraction integral, which is implemented in standard ab initio program. One-electron integral of $V^{\mathrm{ES}}{}_{\mathrm{sr2}}$ can be evaluated in a similar manner to two-electron integral; see Appendix B in page S9. Finally, the one-electron integral of $V^{\mathrm{ES}}{}_{\mathrm{sr2}}$ for the Gaussian functions is represented by eq. S18;

$$\int_{\mathrm{all}} d\mathbf{r}\; g_{Aa}(\mathbf{r})V^{\mathrm{ES}}_{\mathrm{sr2}}(\mathbf{r})g_{Bb}(\mathbf{r}) = \left(\frac{\pi}{\alpha_p}\right)^{\frac{3}{2}} F_{AaBb} \sum_{\mathbf{R},C}^{|\mathbf{r}-\mathbf{r}_C-\mathbf{R}|\le r_{\mathrm{cut}}} \frac{-Z_C}{|\,\mathbf{r}_P-\mathbf{r}_C-\mathbf{R}\,|} \times\mathrm{erf}\left(\sqrt{\frac{\alpha_p\alpha_c}{\alpha_p+\alpha_c}}\,|\mathbf{r}_P-\mathbf{r}_C-\mathbf{R}|\right) \tag{S18}$$

where $\alpha_c = 1/2\sigma^2$. The one-electron integral of $V^{\mathrm{ES}}{}_{\mathrm{sr2}}$ for the Cartesian Gaussian functions is presented in Appendix B (page S9). The one-electron integral of $V^{\mathrm{ES}}{}_{\mathrm{lr}}$ can be evaluated using eqs. S10 and S17.

In this way, the electrostatic interaction between the periodic PC distribution and the one-electron orbital of the embedded cluster model can be correctly evaluated in reasonable computational cost using the super-cell approach, where no approximation is employed except for very large lattice vectors for super-cells. The determination of cut-off energy in Ewald summation method and the dependency on the super-cell size are discussed in page S11.

Appendices for Derivation of One-electron Integral of PE Potential

Appendix A: Fourier transform of product of two Cartesian Gaussian functions

The Fourier transform of product of two Cartesian Gaussian functions is represented as

$$\int_{\text{all}} d\mathbf{r}\ \varphi_{Aal}(\mathbf{r})\varphi_{Bbl'}(\mathbf{r})\, e^{-i\mathbf{G}\cdot\mathbf{r}} \quad = \quad F_{AaBb}\ s_{Ppl_xl'_x}(G_x)\ s_{Ppl_yl'_y}(G_y)\ s_{Ppl_zl'_z}(G_z) \tag{A1}$$

Here, the x-component, $s_{Ppl_xl'_x}(G_x)$, is defined by

$$s_{Ppl_xl'_x}(G_x) \quad = \quad \int_{-\infty}^{+\infty} dx\ (x-x_A)^{l_x}(x-x_B)^{l'_x}\ \exp\left(-\alpha_p|x-x_P|^2\right) e^{-iG_xx} \tag{A2}$$

The y- and z-components, $s_{Ppl_yl'_y}(G_y)$ and $s_{Ppl_zl'_z}(G_z)$, respectively, are similarly defined. Using a binomial expansion, $s_{Ppl_xl'_x}(G_x)$ can be represented as follows:

$$s_{Ppl_xl'_x}(G_x) \quad = \quad \sum_{k=0}^{l_x}\sum_{k'=0}^{l'_x} \begin{pmatrix} l_x \\ k \end{pmatrix} \begin{pmatrix} l'_x \\ k' \end{pmatrix} (x_P-x_A)^{l_x-k}(x_P-x_B)^{l'_x-k'}\ \varphi_{Ppk+k'}(G_x) \tag{A3}$$

Here, $\varphi_{Ppk+k'}(G_x)$ is the x-component of Fourier transform of Cartesian Gaussian function;

$$\varphi_{Ppk+k'}(G_x) \quad = \quad \int_{-\infty}^{+\infty} dx\ (x-x_P)^{k+k'}\ \exp\left(-\alpha_p|x-x_P|^2\right) e^{-iG_xx} \tag{A4}$$

which can be derived using the following recursion relations in a similar manner to eq. 46 of Ref. S2:

$$
\begin{aligned}
\varphi_{Pp\,0}(G_x) &= \left(\frac{\pi}{\alpha_p}\right)^{\frac{1}{2}} \exp\left(-\frac{G_x^2}{4\alpha_p}\right) e^{-iG_x x_P} \\
\varphi_{Pp\,1}(G_x) &= -\frac{iG_x}{2\alpha_p}\,\varphi_{Pp\,0}(G_x) \\
&\;\vdots \\
\varphi_{Ppl_x}(G_x) &= \frac{l_x-1}{2\alpha_p}\,\varphi_{Ppl_x-2}(G_x) - \frac{iG_x}{2\alpha_p}\,\varphi_{Ppl_x-1}(G_x)
\end{aligned} \tag{A5}
$$

The y- and z-components of Fourier transform of Cartesian Gaussian function are similarly derived.

Appendix B: One electron integral of $V_{\mathbf{sr2}}^{\mathbf{ES}}$ in Ewald summation method

In the Ewald summation method, the electrostatic potential of point charges is represented as the sum of two short-range terms and one long-range term, as represented in eq. S14. The second short-range term $V_{\mathrm{sr2}}^{\mathrm{ES}}$ (eq. S16) can be expressed as follows:

$$
\begin{aligned}
V_{\mathrm{sr2}}^{\mathrm{ES}}(\mathbf{r}) &= \sum_{\mathbf{R},C}^{|\mathbf{r}-\mathbf{r}_C-\mathbf{R}|\le r_{\mathrm{cut}}} \frac{-Z_C}{|\,\mathbf{r}-\mathbf{r}_C-\mathbf{R}\,|}\mathrm{erf}\left(\frac{1}{\sqrt{2}\sigma}|\mathbf{r}-\mathbf{r}_C-\mathbf{R}|\right) \\
&= \sum_{\mathbf{R},C}^{|\mathbf{r}-\mathbf{r}_C-\mathbf{R}|\le r_{\mathrm{cut}}} (-Z_C)\left(\frac{1}{2\pi\sigma^2}\right)^{\frac{3}{2}} \int_{\mathrm{all}} d\mathbf{r}'\, \frac{\exp\left(-\frac{1}{2\sigma^2}|\,\mathbf{r}'-\mathbf{r}_C-\mathbf{R}\,|^2\right)}{|\,\mathbf{r}-\mathbf{r}'\,|}
\end{aligned} \tag{B1}
$$

As presented in eq. B1, $V_{\mathrm{sr2}}^{\mathrm{ES}}$ of the Ewald summation method can be regarded as the electrostatic potential formed by the Gaussian charge densities (for more details of the Ewald summation method, see Ref. S3). Thus, one-electron integral of $V_{\mathrm{sr2}}^{\mathrm{ES}}$ can be evaluated in a similar manner to evaluation of two-electron integral which is carried out by the two Gaussian basis functions with the same electron coordinate ($\mathbf{r}'$), the same position ($\mathbf{r}_C + \mathbf{R}$), the same Gaussian width ($\sqrt{2}\sigma$), the same normalization constant ($(1/2\pi\sigma^2)^{3/4}$), and no Cartesian angular momenta ($l_x = l_y = l_z = 0$). Using a Hermite polynomial expansion with Rodrigues' formula,[S4] the one-electron integral of $V_{\mathrm{sr2}}^{\mathrm{ES}}$ for the

Cartesian Gaussian functions is presented as

$$\int_{\text{all}} d\mathbf{r}\, \varphi_{Aal}(\mathbf{r}) V_{\text{sr2}}^{\text{ES}}(\mathbf{r}) \varphi_{Bbl'}(\mathbf{r}) = F_{AaBb} \sum_{\mathbf{R},C}^{|\mathbf{r}-\mathbf{r}_C-\mathbf{R}|\leq r_{\text{cut}}} \left(\frac{\alpha_c}{\pi}\right)^{\frac{3}{2}} \frac{-Z_C \pi^{\frac{5}{2}}}{\alpha_p \alpha_c \sqrt{\alpha_p + \alpha_c}}$$
$$\times \sum_{s_x s_x' t_x t_x' u_x v_x} I_x \sum_{s_y s_y' t_y t_y' u_y v_y} I_y \sum_{s_z s_z' t_z t_z' u_z v_z} I_z$$
$$\times 2B_\nu \left(\frac{\alpha_p \alpha_c}{\alpha_p + \alpha_c} |\mathbf{r}_P - \mathbf{r}_C - \mathbf{R}|^2 \right) \tag{B2}$$

Here, $\alpha_c = 1/2\sigma^2$, B_ν is the ν-th order Boys function as

$$B_\nu(T) = \int_0^1 dt\, t^{2\nu} \exp\left(-Tt^2\right) \tag{B3}$$

and

$$\sum_{s_x s_x' t_x t_x' u_x v_x} I_x = \frac{(-1)^{l_x + l'x} l_x!\, l_x'!}{p^{l_x + l_x'}} \sum_{s_x=0}^{[l_x/2]} \sum_{s_x'=0}^{[l_x'/2]} \sum_{t_x=0}^{l_x - 2s_x} \sum_{t_x'=0}^{l_x' - 2s_x'} \sum_{u_x=0}^{[(t_x + t_x')/2]} \frac{(-1)^{t_x' + u_x} (t_x + t_x')!}{4^{s_x + s_x' + u_x} s_x! s_x'! t_x! t_x'! u_x!}$$
$$\times \frac{a^{t_x' - s_x - u_x} b^{t_x - s_x' - u_x} p^{2(s_x + s_x') + u_x} (r_{Ax} - r_{Bx})^{t_x + t_x' - 2u_x}}{(l_x - 2s_x - t_x)!(l_x' - 2s_x' - t_x')!(t_x + t_x' - 2u_x)!}$$
$$\times \sum_{v_x=0}^{[\mu_x/2]} \frac{(-1)^{v_x} \mu_x! (pc/(p+c))^{\mu_x - v_x} (r_{Px} - r_{Cx})^{\mu_x - 2v_x}}{4^{v_x} v_x! (\mu_x - 2v_x)!} \tag{B4}$$

where $\mu_x = l_x + l_x' - 2(s_x + s_x') - (t_x + t_x')$, $\nu = \mu_x + \mu_y + \mu_z - (v_x + v_y + v_z)$, and I_y and I_z are similarly defined in terms of y- and z-components, respectively. Boys function can be evaluated as

$$B_\nu(T) = \frac{(2\nu)!}{2\nu!} \left[\frac{\sqrt{\pi}}{4^\nu T^{\nu+1/2}} \text{erf}(\sqrt{T}) - e^{-T} \sum_{k=0}^{\nu-1} \frac{(\nu - k)!}{4^k (2\nu - 2k)! T^{k+1}} \right] \tag{B5}$$

when $T > 0$, and $B_\nu(T) = 1/(2\nu + 1)$ when $T = 0$.[S4]

Effects of Cut-off Energy in the Ewald Summation Method and Super-cell Size on Interactions of Rh_2 with Al_2O_3 and $AlPO_4$

Effects of cut-off energy in the Ewald summation method on interactions of Rh_2 with Al_2O_3 and $AlPO_4$:

Because the long-range term of electrostatic potential in the Ewald summation method (eq. S17) quickly converges in reciprocal-space, the cut-off energy E_{cut}, which determines the number of wave-vectors used in Fourier expansion, can be significantly reduced. Figure S1 shows the convergence behavior of total energies of the Al_2O_3 cluster model with respect to cut-off energy value in the presence and absence of the Ewald summation method. Here, a $2 \times 2 \times 1$ super-cell ($33 \times 34 \times 36$ Å), a convergence parameter of $\sigma = 1$ Å, and a real-space cut-off criteria, $(\alpha_p \alpha_c/(\alpha_p + \alpha_c))|\mathbf{r}_P - \mathbf{r}_C - \mathbf{R}|^2 \leq r_{\text{cut}} = 20 \ln 10$, were used; the cut-off criteria is same as the default used in GAMESS[S5] for calculation of one-electron integrals. In the absence of the Ewald summation method, the total energy varies by more than 50 eV when the cut-off range is 400 to 800 eV. In the presence of the Ewald summation method, on the other hand, the total energy converges rapidly with respect to the cut-off energy; for instance, it varies within 0.001 eV when the cut-off energy is larger than 150 eV. Therefore, the cut-off energy of 150 eV was used in this work.

Effect of super-cell size on interactions of Rh_2 with Al_2O_3 and $AlPO_4$:

In the embedding method incorporating periodic electrostatic potential developed in this work, two-electron integrals (Coulomb and exchange integrals) between clusters located at different cells are not considered. Therefore, the large super-cell should be employed so as that the two-electron integrals between clusters located at different cells are negligible.

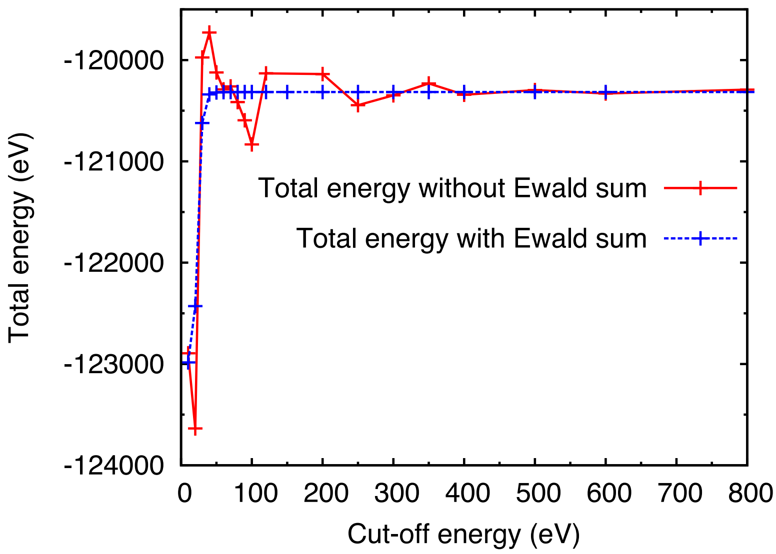

Figure S1: Total energy of Al_2O_3 cluster model as a function of cut-off energy with and without the Ewald summation method (blue dashed- and red solid-lines, respectively).

Table S1 shows dependency of interaction energy and HOMO–LUMO gap on size of super-cell in the Al_2O_3 and $AlPO_4$ cluster models. For the Al_2O_3 cluster model, the interaction energy and HOMO–LUMO gap of the 2×2 super-cell agree with those of the larger ones within 0.02 eV. For the $AlPO_4$ one, those values of the 3×3 super-cell agree with those of the larger ones within 0.01 eV. Therefore, we employed these super-cell sizes in this work.

Table S1: The minimum atomic distances ($d_{\mathbf{min}}$) between clusters located at different cells, interaction energies ($E_{\mathbf{int}}$) of $\mathbf{Rh_2}$ with $\mathbf{Al_2O_3}$ and $\mathbf{AlPO_4}$, and HOMO–LUMO gaps ($\varepsilon_{\mathbf{gap}}$) of distorted surfaces at various sizes of super-cells.

Size of super-cell		1×1	2×2	3×3	4×4	5×5
				Rh_2/Al_2O_3		
d_{min}	(Å)	5.46	22.3	39.1	55.9	72.6
				PBE		
E_{int}	(eV)	^{a}	−6.02	−6.02	−6.02	−6.02
$\varepsilon_{\mathrm{gap}}$	(eV)	^{a}	1.82	1.82	1.82	1.82
				B3LYP		
E_{int}	(eV)	−5.43	−5.50	−5.50	−5.50	−5.50
$\varepsilon_{\mathrm{gap}}$	(eV)	2.44	3.51	3.50	3.49	3.49
				$Rh_2/AlPO_4$		
d_{min}	(Å)	1.69	18.2	34.9	51.6	68.2
				PBE		
E_{int}	(eV)	^{a}	−5.74	−5.71	−5.70	−5.70
$\varepsilon_{\mathrm{gap}}$	(eV)	^{a}	0.63^{b}	0.63^{c}	0.63^{c}	0.63^{c}
				B3LYP		
E_{int}	(eV)	^{a}	−5.57	−5.54	−5.53	−5.53
$\varepsilon_{\mathrm{gap}}$	(eV)	^{a}	2.32^{b}	2.32^{c}	2.32^{c}	2.32^{c}

^{a} SCF calculations do not converge.
^{b} $\varepsilon_{\mathrm{gap}} = \varepsilon_{\mathrm{LUMO}} - \varepsilon_{\mathrm{HOMO\text{-}4}}$.
^{c} $\varepsilon_{\mathrm{gap}} = \varepsilon_{\mathrm{LUMO}} - \varepsilon_{\mathrm{HOMO\text{-}2}}$.

Table S2: Effects of choice of atomic charge on interaction energies (E_{int}; eV) of Rh_2 with Al_2O_3 and $AlPO_4$.

	VLP[a]		PE[b]	
	Bader[c]	Formal[d]	Bader[c]	Formal[d]
	Rh_2/Al_2O_3			
	PBE			
E_{int}	−5.99	−6.79	−6.02	−6.72
	(−4.93)[e]	(−5.20)[e]	(−4.95)[e]	(−5.23)[e]
	B3LYP			
E_{int}	−5.51	−6.18	−5.47	−6.16
	(−4.53)[e]	(−4.81)[e]	(−4.47)[e]	(−4.76)[e]
	$Rh_2/AlPO_4$			
	PBE			
E_{int}	−5.55	−5.44	−5.71	−5.62
	(−5.09)[e]	(−4.99)[e]	(−5.25)[e]	(−5.16)[e]
	B3LYP			
E_{int}	−5.43	−5.32	−5.52	−5.45
	(−4.95)[e]	(−4.85)[e]	(−5.11)[e]	(−5.03)[e]

[a] A number of point charges is 1451940 (920 x 920 x 15 Å^3) for the Al_2O_3 embedded models with very large number of point charges (VLP), and that is 1016310 (970 x 920 x 15 Å^3) for the $AlPO_4$ ones with VLP.

[b] PE indicates periodic electrostatic potential.

[c] The Bader charges calculated by the slab calculations were condidered in the calculation.

[d] Formal charges were considered in the calcilation; +3 for Al, −2 for O, and +5 for P.

[e] In parentheses are the interaction energies after correction of basis set superposition error.

Table S3: Basis set effects on interaction energies (E_{int}; eV) of Rh_2 with Al_2O_3 and $AlPO_4$.

	VLP[a]			PE[b]	
Al	LANL2DZ[c]	SDD[d]	cc-pVDZ[e]	LANL2DZ[c]	SDD[d]
P	LANL2DZ[c]	SDD[d]	cc-pVDZ[e]	LANL2DZ[c]	SDD[d]
O	D95V[f]	DZP[g]	cc-pVDZ[e]	D95V[f]	DZP[g]
Rh	LANL2DZ[c]	SDD[d]	SDD[d]	LANL2DZ[c]	SDD[d]
			Rh_2/Al_2O_3		
			PBE		
E_{int}	−5.99	−6.98	−8.19	−6.02	−7.00
	(−4.93)[h]	(−5.09)[h]	(−5.07)[h]	(−4.95)[h]	(−5.11)[h]
			B3LYP		
E_{int}	−5.51	−6.44	−7.57	−5.47	−6.46
	(−4.53)[h]	(−4.74)[h]	(−4.64)[h]	(−4.47)[h]	(−4.68)[h]
			$Rh_2/AlPO_4$		
			PBE		
E_{int}	−5.55	−5.95	−6.08	−5.71	−6.13
	(−5.09)[h]	(−5.13)[h]	(−5.13)[h]	(−5.25)[h]	(−5.40)[h]
			B3LYP		
E_{int}	−5.43	−5.96	−6.10	−5.52	−5.96
	(−4.95)[h]	(−5.13)[h]	(−5.14)[h]	(−5.11)[h]	(−5.23)[h]

[a] A number of point charges is 1451940 (920 x 920 x 15 Å^3) for the Al_2O_3 embedded models with very large number of point charges (VLP), and that is 1016310 (970 x 920 x 15 Å^3) for the $AlPO_4$ ones with VLP.
[b] PE indicates periodic electrostatic potential.
[c] Los Alamos basis sets and effective core potentials (ECPs) with *d*-polatization function.[S5–S7]
[d] Stuttgart/Dresden basis sets and ECPs.[S8–S10]
[e] Dunning's correlation consistent basis sets.[S11,S12]
[f] Huzinaga-Dunning valence double-zeta basis sets.[S13]
[g] Huzinaga-Dunning double-zeta basis sets with *d*-polarization function.[S13]
[h] In parentheses are the interaction energies after correction of basis set superposition error.

In the case of Rh_2/Al_2O_3, the E_{int} without BSSE correction increases considerably, as the quality of basis sets increases. In the case of $Rh_2/AlPO_4$, the basis set effects on the E_{int} is moderate. In both cases, the E_{int} after BSSE correction depends little on the basis sets, suggesting that the basis set effects arise from the BSSE. Because the E_{int} without BSSE correction calculated with the LANL2DZ is the closest to the E_{int}(no-BSSE), we employed LANL2DZ here for discussing HOMO, LUMO, DOS etc.

Table S4: Cluster size effects on frontier orbital energies ($\varepsilon_{\mathbf{HOMO}}$ and $\varepsilon_{\mathbf{LUMO}}$; eV) and band gaps of distoetd Al_2O_3 and $AlPO_4$.[a]

	VLP[b]	PE[c]	VLP[b]	PE[c]
	distorted Al_2O_3[a]		distorted Al_2O_3-L[a, d]	
	PBE			
$\varepsilon_{\mathrm{LUMO}}$	−5.48	−5.22	−5.57	−5.21
$\varepsilon_{\mathrm{HOMO}}$	−7.29	−7.03	−7.17	−6.80
Band gap[e]	1.81	1.82	1.61	1.59
	B3LYP			
$\varepsilon_{\mathrm{LUMO}}$	−4.83	−4.57	−4.94	−4.58
$\varepsilon_{\mathrm{HOMO}}$	−8.32	−8.08	−8.30	−7.94
Band gap[e]	3.49	3.51	3.35	3.36
	distorted $AlPO_4$[a]		distorted $AlPO_4$-L[a, d]	
	PBE			
$\varepsilon_{\mathrm{LUMO}}$[f]	−8.35	−7.45	−8.47	−7.29
$\varepsilon_{\mathrm{HOMO}}$[f]	−8.98[g]	−8.08[g]	−9.06[g]	−7.89[h]
Band gap[e]	0.63[i]	0.63[i]	0.59[i]	0.60[j]
	B3LYP			
$\varepsilon_{\mathrm{LUMO}}$[f]	−7.84	−6.97	−7.97	−6.84
$\varepsilon_{\mathrm{HOMO}}$[f]	−10.17[g]	−9.29[g]	−10.24[g]	−9.13[h]
Band gap[e]	2.33[i]	2.32[i]	2.27[i]	2.29[j]

[b] These geometries were taken to be the same as the corresponding moiety of Rh_2/Al_2O_3 and $Rh_2/AlPO_4$ optimized by the slab calculations.

[b] A number of point charges is 1451940 (920 x 920 x 15 Å^3) for the Al_2O_3 embedded models with very large number of point charges (VLP), and that is 1016310 (970 x 920 x 15 Å^3) for the $AlPO_4$ ones with VLP.

[c] PE indicates periodic electrostatic potential.

[d] Rh_2/Al_2O_3-L and $Rh_2/AlPO_4$-L mean $Rh_2/(Al_2O_3)_{18}$ and $Rh_2/(AlPO_4)_{19}$ cluster models, respectiveky.

[e] Band gap is $\varepsilon_{\mathrm{LUMO}} - \varepsilon_{\mathrm{HOMO}}$ unless caution is presented as superscript.

[f] Frontier orbitals similar to HO and LU bands of the slab model.

[g] HOMO−2.

[h] HOMO−4.

[i] $\varepsilon_{\mathrm{LUMO}} - \varepsilon_{\mathrm{HOMO-2}}$.

[j] $\varepsilon_{\mathrm{LUMO}} - \varepsilon_{\mathrm{HOMO-4}}$.

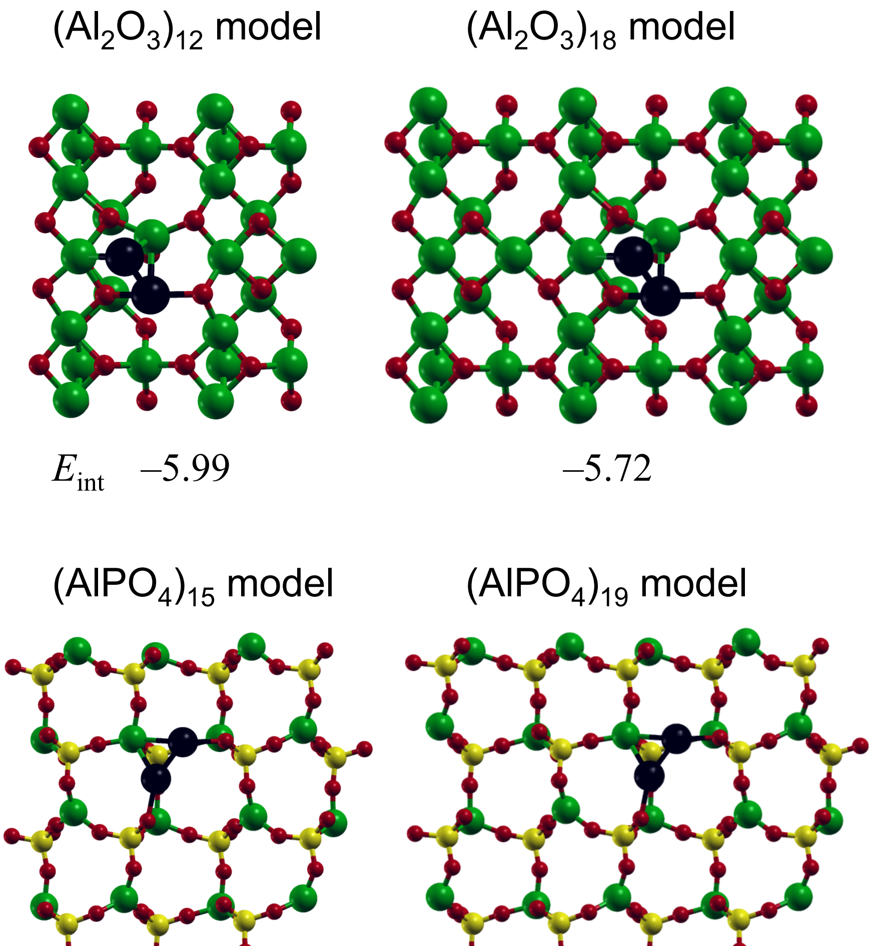

Figure S2: Cluster size effects on interaction energies (E_{int}; eV)[a] of Rh_2 with Al_2O_3 and $AlPO_4$.

[a] PBE functional was used. The embedded cluster model with VLP charges was employed.

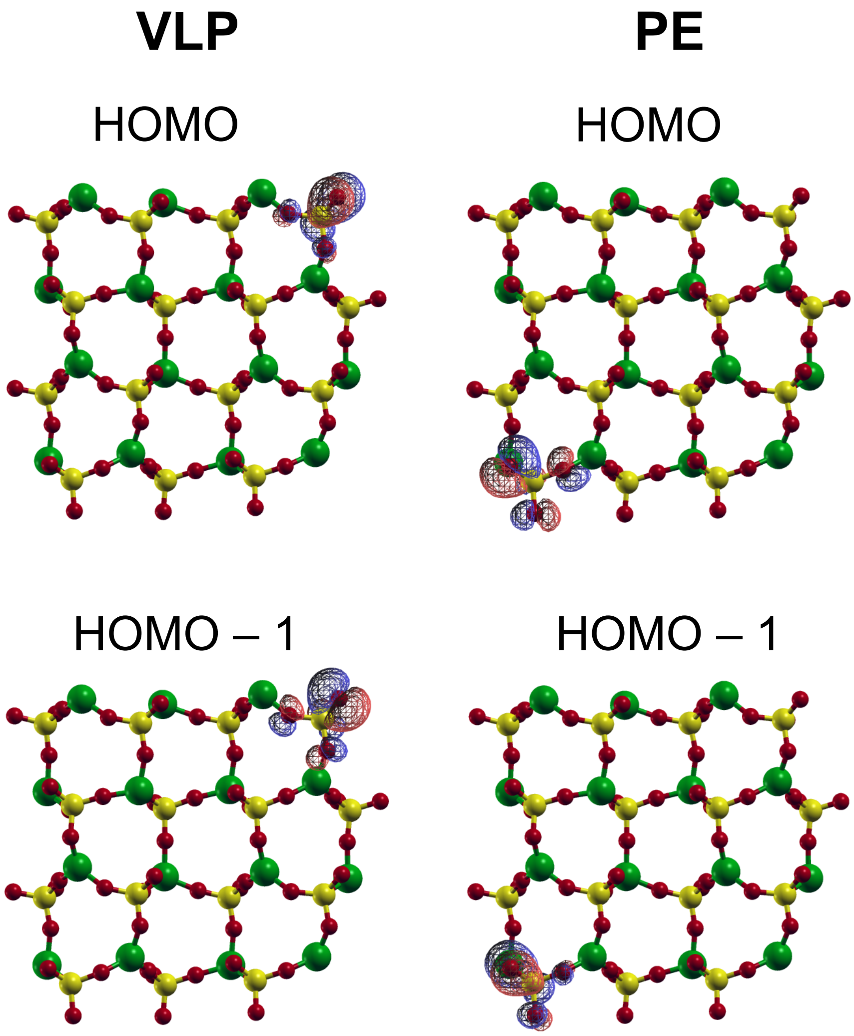

Figure S3: HOMO and HOMO−1 of the $Rh_2/AlPO_4$ cluster models with VLP and PE.

These HOMO and HOMO−1 are localized on the edge, which correspond to the artificial dangling bond. These orbitals cannot be compared with the HO band of the slab model.

References

(S1) Matsui, M. Role of Interchain Interaction in Determining the Band Gap of Trigonal Selenium: A Density Functional Theory Study with a Linear Combination of Bloch Orbitals. *J. Phys. Chem. C* **2014**, *118*, 19294–19307.

(S2) Yu, K.; Libisch, F.; Carter, E. A. Implementation of Density Functional Embedding Theory within the Projector-Augmented-Wave Method and Applications to Semiconductor Defect States. *J. Chem. Phys.* **2015**, *143*, 102806.

(S3) Frenkel, D.; Smit, B. *Understanding Molecular Simulation (Second Edition)*; Academic Press: San Diego, 2002; pp 291 – 320.

(S4) Petersson, T.; Hellsing, B. A Detailed Derivation of Gaussian Orbital-Based Matrix Elements in Electron Structure Calculations. *Eur. J. Phys.* **2010**, *31*, 37.

(S5) Francl, M. M.; Pietro, W. J.; Hehre, W. J.; Binkley, J. S.; Gordon, M. S.; DeFrees, D. J.; Pople, J. A. Self-Consistent Molecular Orbital Methods. XXIII. A Polarization-Type Basis Set for Second-row Elements. *J. Chem. Phys.* **1982**, *77*, 3654–3665.

(S6) Wadt, W. R.; Hay, P. J. Ab Initio Effective Core Potentials for Molecular Calculations. Potentials for Main Group Elements Na to Bi. *J. Chem. Phys.* **1985**, *82*, 284–298.

(S7) Hay, P. J.; Wadt, W. R. Ab Initio Effective Core Potentials for Molecular Calculations. Potentials for K to Au Including the Outermost Core Orbitals. *J. Chem. Phys.* **1985**, *82*, 299–310.

(S8) Igel-Mann, G.; Stoll, H.; Preuss, H. Pseudopotentials for Main Group Elements (IIIa through VIIa). *Mol. Phys.* **1988**, *65*, 1321–1328.

(S9) Bergner, A.; Dolg, M.; Küchle, W.; Stoll, H.; Preuß, H. Ab Initio Energy-Adjusted Pseudopotentials for Elements of Groups 13–17. *Mol. Phys.* **1993**, *80*, 1431–1441.

(S10) Andrae, D.; Häußermann, U.; Dolg, M.; Stoll, H.; Preuß, H. Energy-Adjusted Ab Initio Pseudopotentials for the Second and Third Row Transition Elements. *Theor. chim. acta* **1990**, *77*, 123–141.

(S11) Woon, D. E.; Dunning Jr., T. H. Gaussian Basis Sets for Use in Correlated Molecular Calculations. III. The Atoms Aluminum through Argon. *J. Chem. Phys.* **1993**, *98*, 1358–1371.

(S12) Dunning Jr., T. H. Gaussian Basis Sets for Use in Correlated Molecular Calculations. I. The Atoms Boron through Neon and Hydrogen. *J. Chem. Phys.* **1989**, *90*, 1007–1023.

(S13) Schaefer III, H. F., Ed. *Methods of Electronic Structure Theory*; Modern Theoretical Chemistry; Plenum Press: New York, 1977; Vol. 3.

62

gamma-Al2O3(001) Rh2/Al24O36

Al	8.762850784296630	6.275025008240084	6.1279681070768271
Al	5.930401363024095	4.924749647065852	6.8504232953946221
Al	5.862170448509959	7.686850024882931	6.8181361829093081
Al	6.261511754819407	6.270951510325323	4.0205941476614381
Al	8.738969075823874	14.721584448759794	6.1278569739494171
Al	7.498401831506978	9.018402773918115	4.9503995030555091
Al	7.461339382117327	11.987557633541403	4.8983110478741031
Al	5.907080892821233	13.309703073126098	6.8283030561272681
Al	5.904721906302870	16.063841061850120	6.8508679242636721
Al	9.055418794193097	11.220226532837147	7.0305111117095941
Al	6.260952086372366	14.730865736737613	4.0193907510879411
Al	6.231863485548383	10.478632059477507	7.3332760181282511
Al	14.385440210789946	6.278591503893326	6.1220479671739091
Al	11.533580725746148	4.872044611990028	6.8616970143095741
Al	11.704365122915316	7.562123380849910	6.9489445619424861
Al	11.848630555950944	6.305151364128190	4.0426040017948571
Al	14.343665085109350	14.711434707150605	6.1240882823593491
Al	13.187324134733782	9.010303928876978	4.9712206178921121
Al	13.178283008177440	11.968177096259780	4.9664325691416481
Al	11.602247839055181	13.379251159394586	6.8554162502799141
Al	11.498986459446359	16.086538887723211	6.8508350732380861
Al	14.732593093471912	10.494228748535971	6.9500181759056031
Al	11.850153318181116	14.696514821946490	4.0248207099119741
Al	11.906693552438496	10.457144281541254	7.0417869474174031
O	10.332685305405896	6.287405534367787	7.0629850463509541
O	7.221123689770146	6.263983771580422	7.1374454410748781
O	8.839093095398210	7.706876920071048	5.0057908270670271
O	8.869688207339342	4.907687251415568	4.9720409499754741
O	6.166324519808304	7.714138823460740	5.0293817180335261
O	6.226786311997744	4.829840279594545	5.0730622353998101
O	10.300885526414627	14.694495470233164	7.0464586969538831
O	8.974627305696030	10.591109131271264	5.2351668390750151
O	7.204760647612241	14.717718376592881	7.1509298772701921
O	6.295614373440485	10.499155754639215	5.0314196778761271

O	10.690894289380708	11.858411032826920	7.3347978088918501
O	11.017620199961813	9.019879367250768	7.7882163467430091
O	8.863277623169965	16.092356678187890	4.9749583881887631
O	8.819170879904139	13.309447449789429	4.9980151643780741
O	7.414631251417997	11.961198267000304	6.8726889881758551
O	7.252285536362678	8.980971487913052	6.8951317675229301
O	6.226791450154687	16.163373108438648	5.0802144527358161
O	6.161678402477171	13.287211478933864	5.0382120288740671
O	4.702592262651906	6.285471743784201	7.0600785271757301
O	12.883948750419218	6.202673494476930	7.1986398940379481
O	14.451896442425268	7.665419789650470	4.9678788789372561
O	14.451230230049461	4.897948128585901	4.9759009193422851
O	11.840181550924667	7.723979013035787	5.1488564456212781
O	11.816430551457355	4.850491199039271	5.0833847235304681
O	4.697196271256240	14.695013378889559	7.0608282289528681
O	14.555420174324345	10.519331591207798	5.1177404028335901
O	12.822182780854586	14.733731647948625	7.1726715466297761
O	11.860215633755196	10.471428424288005	5.1060522783443411
O	4.933995154292224	11.781836699536083	7.3580386486880501
O	4.847374466521948	9.239379742470099	7.3505519136598851
O	14.441909236268254	16.090453281993135	4.9756792939591081
O	14.439870121009760	13.320000551679428	4.9811269090296821
O	13.208886568144887	11.766666377719119	6.9705420129103711
O	13.297706986281600	9.222427330587724	6.9075741452731561
O	11.812407252697401	16.140146309361469	5.0795337459725541
O	11.829350286801606	13.252976821392307	5.0817055554916671
Rh	9.006952887035229	8.985329177369747	7.8697270883165270
Rh	8.006343672079991	10.455969405033512	9.3744636192809080

92

tridymite-AlPO4(110) Rh2/Al15P15O60

Al	7.195031995533290	5.374328311695990	3.740513561850480
Al	1.661064074965470	5.383193114405330	7.917290535486850
Al	7.271017408427600	5.325169195876190	11.987924149877999
Al	1.650561292017710	5.377270429230070	16.217187099247699
Al	10.402355258891699	5.342536207024110	7.818324932969820

Al	16.067572940286400	5.353627895579700	12.068630814087999
Al	10.451913096305701	5.367854373933560	16.229809471476901
Al	3.308890443857070	7.801714105130000	3.485931351331900
Al	6.060701949481110	8.079099085136900	7.865428727205260
Al	3.109643438648130	7.753214151903370	11.527878094954700
Al	5.634694059913850	7.784608766464950	15.847853466093500
Al	11.989462435997501	7.763350529539670	3.270428860478190
Al	14.559959512757899	7.778052187679800	7.417926568879930
Al	12.077939069956800	7.777238985322110	11.752879420548799
Al	14.569059019397899	7.805522910303510	15.819315037175800
P	1.570842329843540	5.340002187111240	4.671739621415670
P	7.282290841320010	5.304791122867480	8.736963750304239
P	1.528875245087100	5.334286387371280	12.989153007557700
P	10.340661012676300	5.332441929428930	4.607237763926910
P	16.169821107961301	5.326882584330440	8.812030285580599
P	10.365526105279899	5.332123606268550	12.992095286869800
P	6.128272112709680	8.063008081221280	4.641913924610190
P	2.868228667335630	8.018875456154751	8.564060346614660
P	5.943006097455970	8.068000437162770	12.818834921244100
P	14.843588335314299	8.056878347437140	4.440867542422490
P	11.671732321144400	8.089349450869671	8.696015865175029
P	14.915774547171599	8.085184470994781	12.855447779770600
P	7.320883510593320	5.333931686566170	17.158734479607489
P	2.781206359559000	8.054663823628760	17.116403618495188
P	11.631453467325400	8.066979243165720	16.952776653220266
O	0.096708540803287	5.507415129922790	4.289908276164780
O	2.078308573727380	3.979747278224040	4.189937899579610
O	2.390076466643400	6.450692159790940	3.969137540389660
O	1.748788820016150	5.491102199038550	6.174133858838130
O	8.726975145222470	5.472964124095390	8.221318295490271
O	6.331324239283420	6.290397692601020	8.071429048745060
O	6.824366003329150	3.873719134157320	8.443440413461170
O	7.306823635931090	5.506188782026850	10.268641886521300
O	0.030272705934572	5.443013811624770	12.714307814732500
O	2.067998686035630	3.974921726525700	12.546145285887199
O	2.237674174269420	6.441767279445140	12.166589499957800

O	1.821612555617350	5.568465724851090	14.472418271350200
O	8.849416618094789	5.446964171164020	4.336795622070060
O	10.888443415915299	3.976637147670530	4.165107969085250
O	11.060804332374101	6.440528569573090	3.789553671512600
O	10.650798830983399	5.560691135429630	6.091882289936840
O	17.617642593402000	5.475608363836370	8.378331230185699
O	15.331976972319600	6.457630708621990	8.140358784440400
O	15.580376865950500	3.986447591994020	8.368916537044630
O	16.034140940698300	5.498028112639540	10.324852636869499
O	8.887681111630339	5.473095362325320	12.650586243822501
O	10.907724367806701	3.982674996818230	12.529874448237100
O	11.138903972179600	6.452005017788660	12.232262978775800
O	10.596965347138100	5.529847125872510	14.485605122051600
O	4.592846119148220	8.441542522942211	4.368521696798000
O	6.098041288915420	6.474567222626160	4.506637672357480
O	7.078584734807900	8.691058673405809	3.694269552449140
O	6.352816920730360	8.397762041833630	6.143081328121590
O	4.330163851637490	8.287376317217880	8.144615774050040
O	1.804722758135440	8.556066899378511	7.686884620908140
O	2.736306847052660	6.441567080999580	8.790695198777740
O	2.782486874145520	8.557291910750690	10.085354590515900
O	4.413172032092060	8.230646098468000	12.520334696698400
O	6.232698817400400	6.547532526340520	12.692222056407500
O	6.801424730542190	8.953524842919480	11.964305489601699
O	6.107766708007870	8.419858591135769	14.336488186429900
O	13.264141019775300	8.232184634352519	4.276629352492140
O	15.022387945354600	6.488616331829790	4.455424749493470
O	15.656968666218500	8.790770407094559	3.459521996323860
O	15.063178126466500	8.475611462805819	5.959717275303750
O	13.118273399990800	8.308815895932479	8.138467358756531
O	10.698873947178200	8.975435442802739	7.972953418731580
O	11.383598843244100	6.567206248597980	8.621118311182590
O	11.771357422643501	8.443299485256460	10.221670075461301
O	13.344811359590100	8.359643064495360	12.700244583802700
O	14.985929397152301	6.504893714877260	12.820379520118500
O	15.767255684652699	8.778820982015599	11.876075714947000

O	15.172936938480900	8.460433197030209	14.371692356229699
O	8.770258154863940	5.486639061937220	16.697693555519727
O	6.488309543534200	6.462220991582590	16.478049720871699
O	6.751597218061890	3.988381114174440	16.706463527331099
O	7.210907381875690	5.500371378548090	18.667680427681777
O	4.246565935153230	8.383598749401990	16.574304584166399
O	1.703494717610860	8.741917693667791	16.385443606759701
O	2.711510963509520	6.473827398876870	17.066794919176314
O	2.903018847982470	8.414407394195459	18.645924655025809
O	13.120738811887600	8.350340661976920	16.481462810954000
O	10.600492276440400	8.719028196397961	16.127754617830000
O	11.533895538471301	6.489271703384880	17.023794380077231
O	11.667983385369300	8.511654963731900	18.476241529820129
Rh	7.222428261131680	9.125149933629411	9.853400258451369
Rh	8.563089356276249	9.148356559392710	8.029911843482680